

Super Continuum Generation at 1310nm in a Highly Nonlinear Photonic Crystal Fiber with a Minimum Anomalous Group Velocity Dispersion

Ashkan Ghanbari¹, Ali Sadr², Hadi Tat Hesari³

1- Department of Electrical Engineering, Qazvin Islamic Azad University, Qazvin, Iran
Email: ghanbari.ashkan@yahoo.com (Corresponding author)

2- Department of Electrical Engineering, Science and Technology University of Iran, Tehran, Iran
Email: sadr@iust.ac.ir

3- Department of Electrical Engineering, Qazvin Islamic Azad University, Qazvin, Iran
Email: h.tat.hesari@qiau.ac.ir

Received: Dec. 2012

Revised: May 2013

Accepted: June 2013

ABSTRACT:

In the present study, we investigate the evolution of the super continuum generation (SCG) through the triangular photonic crystal fiber (PCF) at 1310nm by using both full-vector multi pole method (M.P.M) and novel concrete algorithms: Symmetric Split-step Fourier (SSF) and fourth order Runge Kutta(RK4) which is an accurate method to solve the general nonlinear Schrodinger equation (GNLSE). We propose an ideal solid-core PCF structure featuring a minimum anomalous group velocity dispersion (GVD), small higher order dispersions (HODs) and enhanced nonlinearity for appropriate super continuum generation with low input pulse energies over discrete distances of the PCF. We also investigate the impact of the linear and nonlinear effects on the super continuum spectra in detail and compare the results with different status.

KEYWORDS: Photonic Crystal Fiber (PCF), Dispersion, Silica, Multi pole, Super Continuum.

1. INTRODUCTION

Since the various nonlinear applications of the photonic crystal fibers (PCFs) are invaluable in communication fields, in recent years they have been highly considered in scientific studies. The arrangement of the air holes in the cladding region gained more importance due to the optical properties of PCFs such as highly nonlinearity, large and small mode areas, high numerical aperture, adjustable zero dispersion and so on[1]. To make the effective refractive index and consequently the propagation characteristics of the PCF appropriate for different cases, the cladding's microstructure can be accordingly changed. This change in micro structure can be achieved by making changes into the size of the air holes. The considerable changes of the air hole diameter (d), pitch (Λ), and structure of PCF have helped in tailoring several important optical properties, such as dispersion, effective area and nonlinearity [1] and [2]. For example, it is possible to design highly nonlinear PCFs with two zero dispersion wavelengths (ZDWs) which is important specially in the nonlinear applications (particularly super continuum generation and optical pulses compression) or the PCFs with a small core design can cause the zero dispersion

wavelengths to be shifted to the wavelengths which are significantly shorter than the ZDW of the conventional fibers [1]-[3]. At the same time, the relatively low nonlinearity of silica is neutralized by the small effective area of the PCF that gives a very nonlinear response to low pump energy (exclusively with the design of small hole pitch and large normalized air holes size). However, these particular properties have made photonic crystal fiber an ideal candidate for nonlinear applications like SCG or soliton effect of optical pulses compression. Broadband light sources based on super continuum generation have already found applications in various fields such as spectroscopy, military applications and so on [1], [3] and [4]. Recently, SC - generation based on silica PCFs with various geometrical structures have been generated in different wavelength regions in the range of 800nm, 850nm or 1550nm [1-4]. However, according to our researches, the SC-generation of low-energy 1310nm in highly nonlinear PCF structures and the impact of the linear and nonlinear effects on the super continuum generation have not been studied so far. Thus, in this paper, we focus on the silica PCF design for a broadband SC- generation in the 1310nm region. The design of PCF is presented and it is shown

through numerical results that, the proposed PCF structure is suitable for the efficient SC generation with a slight required energy in this applicable low loss telecommunication wavelength and then we study the super continuum generation and the impact of the dispersion and nonlinear effects on it in detail.

2. DISPERSION ENGINEERING OF THE PROPOSED PCF

Dispersion affects the Ultra short pulses propagation in a way that leads to broadening the pulse in the time domain. Hole pitch (Λ), wavelength (λ), and normalized air holes diameter ($\frac{d}{\Lambda}$) are three factors on which photonic crystal fibers dispersion depends [1] and [2]. The dependency of the group velocity dispersion on the wavelength, pitch (Λ), and normalized air holes diameter ($\frac{d}{\Lambda}$) allows to shift the zero dispersion point [1-6]. Silica owns well-known optical properties and is one of the most important materials for fabrication of the optoelectronic devices [1], [2]. As seen in Figure 1, we consider a conventional silica photonic crystal fiber with a triangular lattice of circular and six equally spaced air holes, where d is the hole diameter, Λ is the hole pitch, MN_r is the number of missing rings in the center of the PCF, N_r is the number of rings ($N_r = 6$ is considered here). The refractive index of the silica is considered to be 1.45. In the center, an air hole is omitted ($MN_r = 1$) creating a central high index defect acting as the fiber core [5], [6].

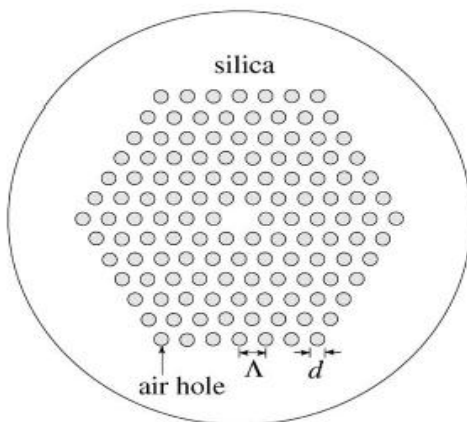


Fig. 1. Silica- PCF schematic [5]

The total dispersion in the PCFs is calculated from the following formula [5-7],

$$D_t(\lambda) = \frac{-\lambda \partial^2 \text{Re}[n_{eff}(\lambda)]}{c \partial \lambda^2} + \frac{-\lambda \partial^2 n_s(\lambda)}{c \partial \lambda^2} \quad (1)$$

D_w D_m

Where, n_s , is the refractive index of pure silica (or any other materials), λ is the corresponding wavelength, c is the velocity of light in a vacuum and n_{eff} is the effective refractive index. Full-vector multi pole method (M.P.M) can be used to analyze the dispersion properties of the silica PCFs. To achieve this purpose, we use the CUDOS MOF software¹ which solves the mode equation obtained from Maxwell equations, using multi pole method and is a common software for designing PCFs. By implementation of the general data relevant to the fiber in the software such as the number of the missing air holes, the number of air hole rings, wavelengths range, desired hole pitches and hole diameters size, type of material which is used in the fiber and so on, we can calculate the values of the effective refractive index, n_{eff} , for different wavelengths. As seen in (1), the waveguide dispersion (D_w) has to be added to the material dispersion (D_m) to obtain the total dispersion. In the case of pure silica, n_s , can be directly derived from the sellmeier formula as below [5] and [8]:

$$n_s^2(\lambda) = \frac{0.696166\lambda^2}{\lambda^2 - 0.0684043^2} + \frac{0.4079426\lambda^2}{\lambda^2 - 0.1162414^2} + \frac{0.897479\lambda^2}{\lambda^2 - 9.896161^2} + 1 \quad (2)$$

The GVD of the PCF is then can be calculated directly by (3) [9],

$$GVD(\beta_2)(\lambda) = -\frac{\lambda^2}{2\pi c} D_t(\lambda) \quad (3)$$

In Figure 2, we have plotted the GVD as a function of wavelength in the visible and infrared regions of the spectrum for the largest possible value of the normalized air hole size ($\frac{d}{\Lambda} = 0.8$) and different pitches (Λ). There are several notable features as seen in Figure 2. First, there is a minimum and nearly flat region of the negative GVD which is shifted to the higher wavelengths by changing the pitch (Λ). So, by choosing the proper pitch (Λ), this region can be centered at desired wavelengths. As illustrated in

¹. The CUDOS MOF software is licensed and published by university of Sydney

Figure 2, by choosing the values $\Lambda = 1.38\mu\text{m}$ and $\frac{d}{\Lambda} = 0.8$, the minimum and nearly flat region can be centered at 1310 nm. The importance of nearly flat region in super continuum generation is due to its results as smaller higher order dispersions. Second, the dispersion properties of the fiber are highly unusual with two lying zero dispersion wavelengths at 750nm and 1900nm and a large minimum anomalous GVD between these two zero dispersion wavelengths. The PCFs with only one zero dispersion wavelengths in visible or infrared region or with two widely separate zero dispersion wavelengths could be compared to the designed dispersion profile in this paper [10-13]. It is noteworthy that, in this design, we could achieve two zero dispersion wavelengths in the visible and short-wavelength infrared (SWIR) regions of the spectrum respectively. So, as already described in several studies [2], [14], in this situations, by choosing a pump wavelength between two nearly close zero dispersion wavelengths (here at 1310nm), high quality, stable and compressible spectra with a high spectral density and low noise can be generally generated (especially applicable in experimental generations)[14].

When considering the propagation of pulses with femtosecond duration, the third, fourth and fifth-order dispersion will be of the great importance and must be included in the generalized Schrodinger equation (GNLSE). In Figure 3 we have plotted the third order dispersion (TOD) as a function of wavelength in the same regions of the spectrum as GVD for $\frac{d}{\Lambda} = 0.8$ and different pitches. This figure shows that the slight positive TOD ideally required for the SC-generation would be provided by the novel structure PCF in the wavelength region where a minimum and nearly flat anomalous GVD can be found. The fourth and fifth order dispersions are illustrated in Figure 4 and Figure 5 implying that although the higher order dispersions are small in 1310 nm wavelength, they should be considered in the wave equation. The novel designed silica PCF is known to be appropriate for super continuum generation (SCG) according to the fact that the ratio of the higher-order dispersions to the GVD would be small at the 1310 nm wavelength.

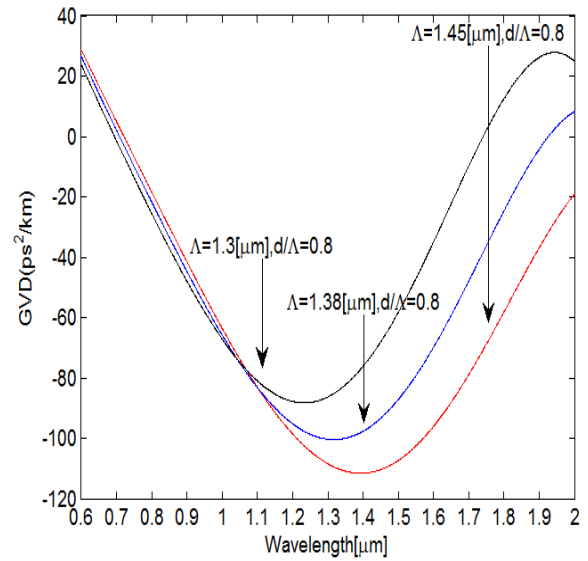


Fig. 2. GVD of PCF as a function of wavelength for $\frac{d}{\Lambda} = 0.8$ and several pitches

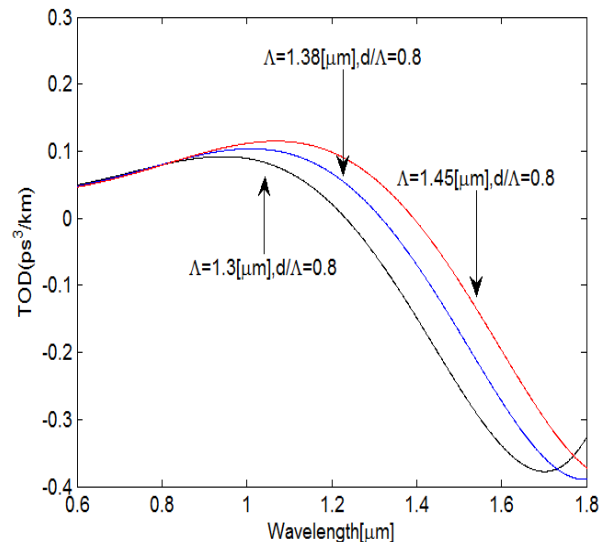


Fig. 3. TOD of PCF as a function of wavelength for $\frac{d}{\Lambda} = 0.8$ and several pitches

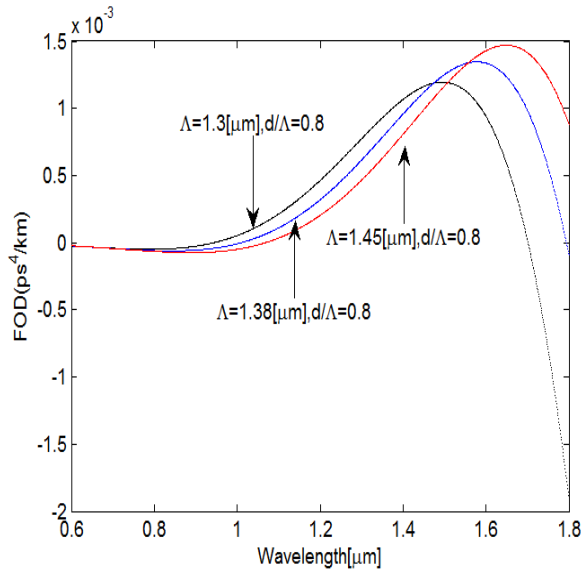


Fig. 4. FOD of PCF as a function of wavelength for $\frac{d}{\Lambda} = 0.8$ and several pitches

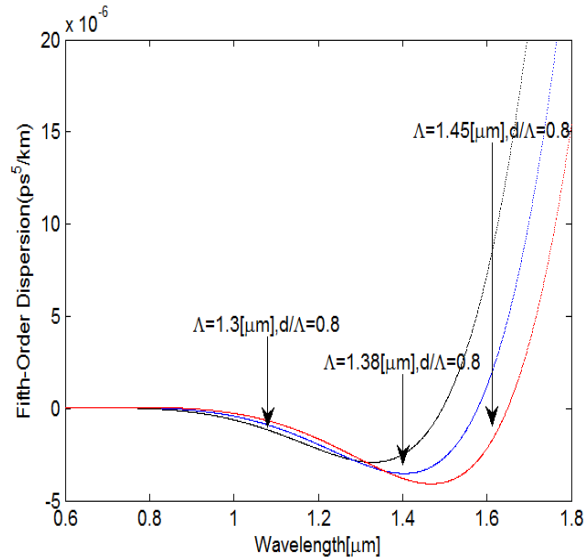


Fig. 5. Fifth –order dispersion of PCF as a function of wavelength for $\frac{d}{\Lambda} = 0.8$ and several pitches

3. THE PROPOSED PCF EFFECTIVE AREA

One of the key factors in designing PCFs is effective mode area (A_{eff}). The effective mode area is related to the effective area of the fiber's core, which is calculated using, [15]

$$A_{eff} = \frac{[\int \int_{-\infty}^{\infty} |F(x, y)|^2 \partial x \partial y]^2}{\int \int_{-\infty}^{\infty} |F(x, y)|^4 \partial x \partial y} \tag{4}$$

Where $F(x, y)$ is the fundamental mode distribution. A smaller effective area leads to an increase in fiber nonlinearity coefficient, higher intensities, a reduction in nonlinear length and finally decreasing the required energy for nonlinear applications such as soliton effect input optical pulses compression and super continuum generation. However, it is conventional to show that the effective area can also be related to the PCF's spot size, w_{PCF} , through $A_{eff} = \pi(w_{PCF})^2$ [15].

In this paper, we have investigated the effective mode area of the proposed PCF structure as a function of wavelength. The effective area of the fundamental mode for our proposed PCF is shown in Figure 6. In this figure it can be noticed that, first, the designed PCF effective area for $\Lambda = 1.38 \mu m$ and $\frac{d}{\Lambda} = 0.8$ at 1310nm

is calculated to be $1.9 \mu m^2$. Secondly, the effective area is so smaller than that of the conventional fibers or standard photonic crystal fibers at 1310nm wavelength up to now [2], [16], [17] and [18]. The PCFs structure with two nearly close zero dispersion and nearly flat GVD have relatively small effective area and would be useful for some nonlinear applications, such as super continuum generation.

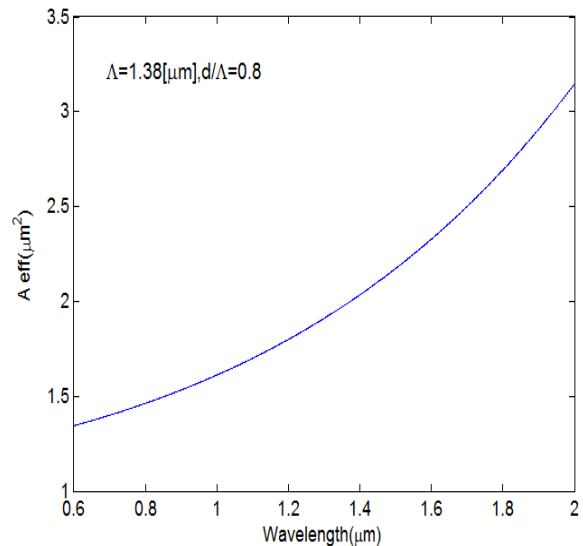


Fig. 6. Effective area of the fundamental mode for silica- PCF as a function of wavelength

4. MODELING THE SUPERCONTINUUM

Modeling of the super continuum generation can be achieved considering the general nonlinear Schrodinger equation (GNLSE) that includes the higher order dispersions (HODs), the Raman effect, the self-steepening, the self-phase modulation (SPM). Such equations can be written as [19] and [20].

$$\begin{aligned} \frac{\partial A}{\partial z} = & -\frac{i\beta_2}{2T_0^2} \frac{\partial^2 A}{\partial t^2} + \frac{\beta_3}{6T_0^3} \frac{\partial^3 A}{\partial t^3} \dots \\ & \dots - \frac{\alpha}{2} + i\gamma(1-f_R)|A|^2 A + \frac{i}{\omega_0} \frac{\partial(|A|^2 A)}{\partial t} + \dots \\ & \dots + i\gamma f_R \left(A \int_0^\infty h_R |A(z, t-t')| dt' + \dots \right. \\ & \left. \dots + \frac{i}{\omega_0} \frac{\partial}{\partial \tau} \left[A \int_0^\infty h_R |A(z, t-t')| dt' \right] \right) \end{aligned} \quad (5)$$

Where, t stands for the reduced time, T_0 as the initial pulse width of optical pulses (note that, in this paper we consider the FWHM value as $T_{FWHM} = 1.76T_0$) and $A(z, t)$ as the pulse amplitude. $\alpha(m^{-1})$ stands for the linear loss coefficient $\beta_2, \beta_3, \beta_4, \beta_5$ are GVD, TOD, FOD, and Fifth-order dispersion respectively. ω_0 stands for the central angular frequency, $s.s = 1/\omega_0$ is responsible for self-steepening and γ stands for the nonlinear coefficient defined by (6),

$$\gamma = \frac{n_2 \omega_0}{c A_{eff}} \quad (6)$$

Where $n_2(m^2/W)$ is the nonlinear refractive index (silica has a nonlinear refractive index of $3.2 \times 10^{-20} m^2/W$), A_{eff} is the modal effective area, and c denotes the speed of light. f_R stands for the relative strength of Kerr and Raman interactions and finally, $h_R(t)$ is the Raman response function [19] and [20]. An analytical form of $h_R(t)$ also exists which is given by (7). Experiments show that, $f_R = 0.18$, $\tau_1 = 12.2fs$ and $\tau_2 = 32fs$ from [1],[19],[20].

$$h_R(t) = \frac{\tau_1^2 + \tau_2^2}{\tau_1 \tau_2} \exp(-t/\tau_2) \sin(-t/\tau_1) \quad (7)$$

Employing the normalized time $\tau = \frac{t}{T_0}$, normalized

distance $\xi = \frac{z}{L_D}$, and the normalized pulse amplitude

$$U(z, \tau) = \frac{N_p A(z, \tau)}{\sqrt{P_0}} \quad (8)$$

$$\begin{aligned} \frac{\partial U}{\partial \xi} = & -\frac{i \operatorname{sgn}(\beta_2)}{2} \frac{\partial^2 U}{\partial \tau^2} + \frac{\beta_3}{6|\beta_2|T_0} \frac{\partial^3 U}{\partial \tau^3} \dots \\ & \dots - \frac{\alpha L_D}{2} U + i\bar{N}U - \frac{i}{\omega_0 T_0} \frac{\partial(\bar{N}U)}{\partial \tau} \end{aligned} \quad (8)$$

Where, N_p is soliton order ($N_p = (\frac{\gamma P_0 T_0^2}{|\beta_2|})^{0.5} = 1$ for the fundamental soliton), P_0 implies the peak power of the input pulse, and \bar{N} is defined by (9),

$$\bar{N} = \frac{N_p N(z, \tau)}{P_0} \quad (9)$$

The delayed response $N(z, \tau)$, is defined by, [20] and [21],

$$N(z, \tau) = (1-f_R)|A|^2 + f_R \left(A \int_0^\infty h_R |A(z, \tau-\tau')| d\tau' \right) \quad (10)$$

And L_D is the dispersion length defined by (11),

$$L_D = \frac{T_0^2}{|\beta_2|} \quad (11)$$

The novel concrete algorithms: symmetric split-step Fourier (S-SSFM) and fourth-order Runge Kutta (RK4) is used to simulate the Generalized Nonlinear Schrodinger Equation (GNLSE) which is an accurate method for solving the GNLSE. We also used a chirp-free secant hyperbolic pulse at the input as [19], [22] and [23].

$$U = N[\operatorname{sech}(\tau)] \quad (12)$$

The photonic crystal fiber designed for this work is made of pure silica [24]. The pitch of the fiber is $\Lambda = 1.38 \mu m$ and it has an air hole diameter of $d \approx 1.1 \mu m$. The fiber effective area is $1.9 \mu m^2$. At the wavelength of 1310nm, the high nonlinear coefficient is estimated to be $\gamma = 80(W.Km)^{-1}$, and up to fifth-order chromatic dispersion coefficients are as following,

$$\beta_2(\text{GVD}) = -100 ps^2/km,$$

$$\beta_3(TOD) = 0.004 \text{ ps}^3 / \text{km}$$

$$\beta_4 = 6.4 \times 10^{-4} \text{ ps}^4 / \text{km},$$

$$\beta_5 = -3.04 \times 10^{-6} \text{ ps}^5 / \text{km}.$$

The fiber loss is neglected ($\alpha = 0$) since only a short length of the fiber is considered in the simulations. We also conducted numerical simulations on 176fs (FWHM) secant hyperbolic input pulse ($\approx T_0 = 100\text{fs}$), propagating in the PCF with a peak power of 5280 watt (corresponding to soliton order of $N=6.5$) in the wavelength range typically from 600nm to 2000nm covering the visible and short-wavelength infrared (SWIR) of spectrum.

5. SIMULATION RESULTS

The spectrum evolution of the femtosecond optical pulses at different locations of the PCF is shown in Fig.7 under following conditions: a) the GVD and SPM are the only events occurring in the GNLSE, b) in the presence of full dispersion constants, c) when SRS is also taking into account, d) by considering SS (full β +SRS+SS). The condition in which β_2 (GVD) and SPM are the only occurrences, the spectrum evolves periodically into a symmetric multi-peak structure along the PCF (see figure 7a). In the condition that the higher-order dispersions exist (see figure 7b), subsequently, the focal part of the related spectrum initially broadens on the first distances of the PCF and spread more with further propagation in comparison with previous situation when only SPM and GVD are considered. In this situation, also, the advent of the anti-Stokes frequency components can be mentioned as the most noticeable result.

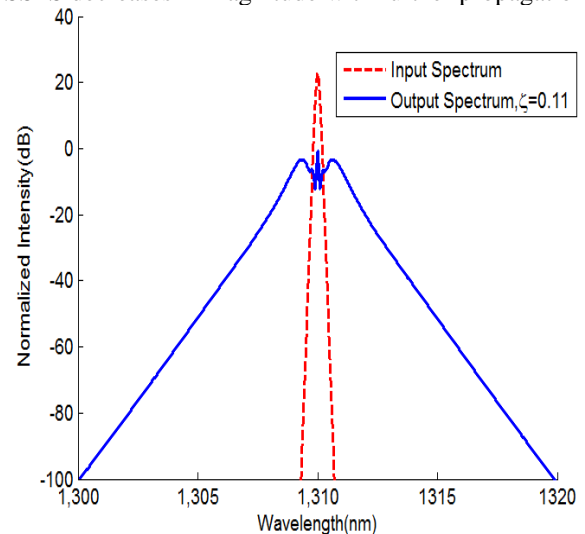
Adding the Raman term in the wave equation results in a huge spreading of the pulse spectrum towards the low frequencies (see figure 7c). Now, by including self-steepening, the amplitude of the blue components will increase and a reduction in the spectrum spreading towards the lower wavelengths will happen (see figure 7d). New anti stokes components (blue components) are also form in the spectrum for further propagation lengths. Figure 8a clearly shows the temporal compression of the input optical pulse to 8 fs Ultra short laser pulse, when all the linear and nonlinear terms included in the GNLSE. It is understood that the Self Phase Modulation (SPM) causes the input pulse relating to a N^{th} order soliton to be compressed in the first few centimeters of the fiber. We can also see slight vibrations at the leading edge of the output compressed pulse due to the effects of the higher order dispersions

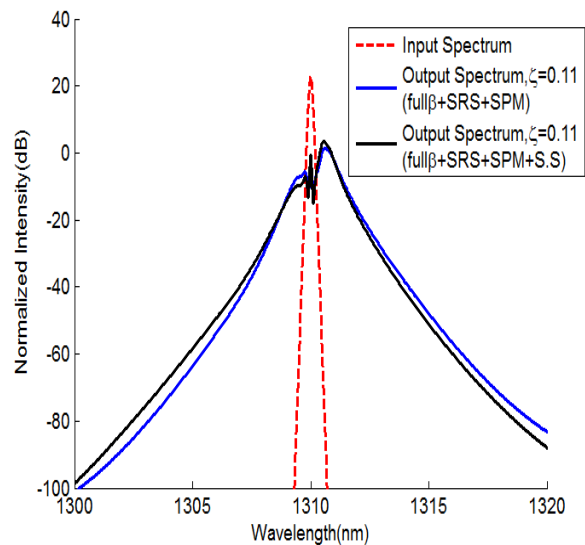
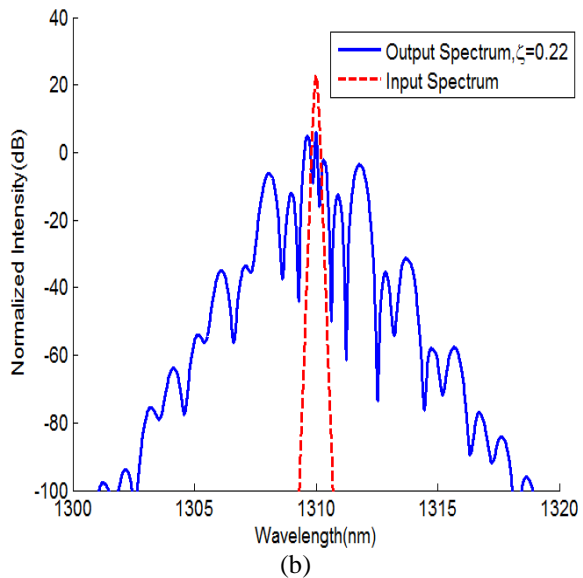
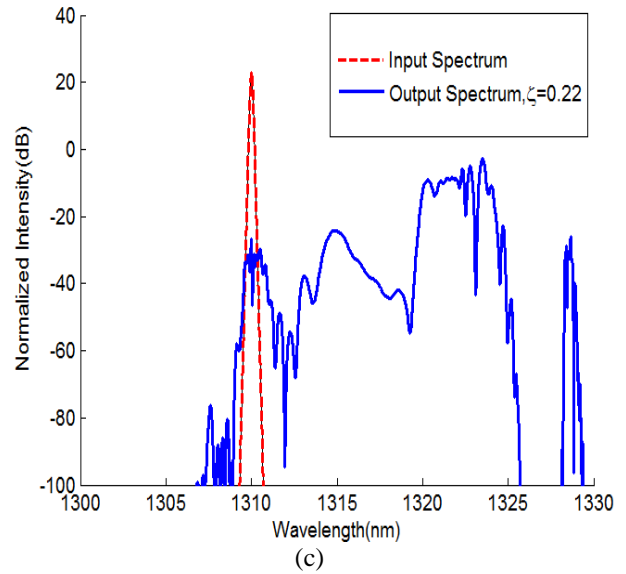
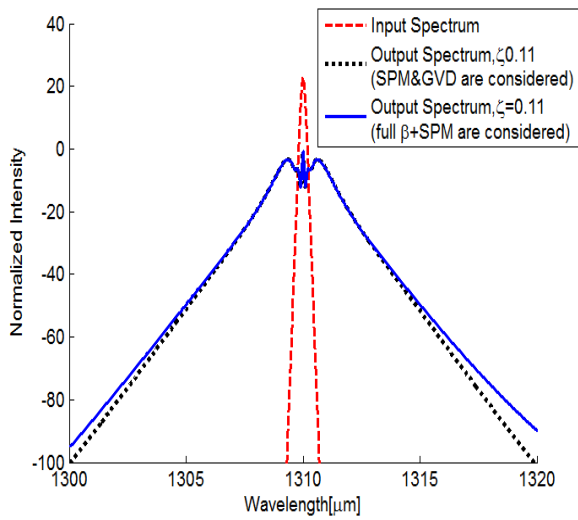
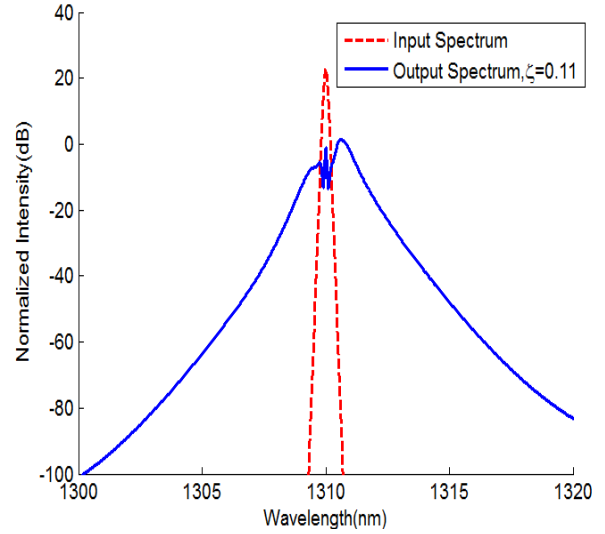
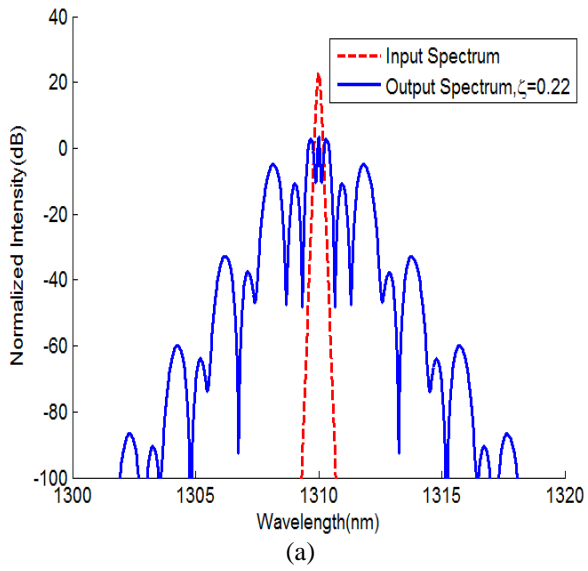
and also a rapid delay of the optical pulse due to the full linear and nonlinear effects.

Figures 8b-c show the amplitudes and width of the multiple fundamental solitons generated through breaking up the N^{th} order soliton due to the perturbation of this soliton by SRS and the higher-order dispersions. This figure also explicitly shows the mentioned break up of the input pulse. Two red and blue parts of the spectra of the multiple solitons respectively overlap with the Raman gain spectrum and the resonant linear waves. Due to these overlaps, the resonant waves reinforce and appear as anti-Stokes (blue) components while SRS is the cause for the red components to reinforce. The method by which SRS amplifies the red components is to shift the central frequency of the solitons farther to the red. As shown in Figures 7c-d, the generated multiple solitons owning different widths, different frequency shifts are applied on them and are emerged as separate stokes peaks in the spectrum. Different frequency shifts which are applied on the solitons, result in distinct group delays which cause them to be indicated as the separate pulses in the time trace.

Figure 8c illustrates that the narrowest soliton experiences the largest shift and consequently the higher delay for the pulses. The frequency shift is commensurate with the length of fiber. Consequently, as the fiber gets longer, the spectrum spreads more towards the lower frequencies.

Through the propagation of the solitons along the PCF, losses and dispersions happen and cause them to broaden by passing the time. Hence, in the long run, the overlap between their spectrum and Raman gain spectrum would not appear and the frequency shift would also stop. In addition, as the solitons shift their central frequency, the nonlinearities get weaker by the Self Steepening. According to the stated reasons, the SSFS decreases in magnitude with further propagation.





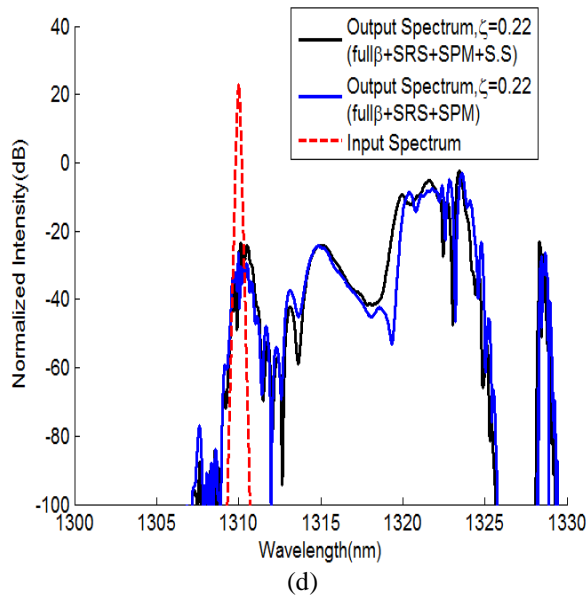


Fig. 7. Simulation of the spectrum at the output of the proposed photonic crystal fiber (PCF) after, $\xi = 0.11$ and $\xi = 0.22$ respectively
 a) Only GVD and SPM are considered
 b) Full β + SPM are considered
 c) full β + SRS + SPM are considered, and
 d) full β + SPM + SRS + S.S are considered

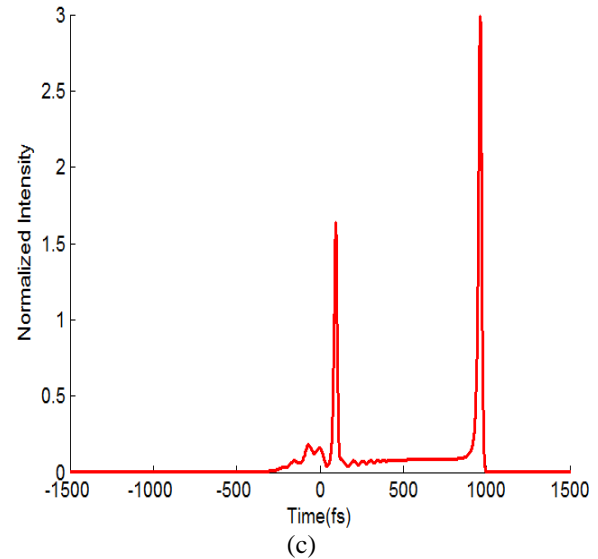
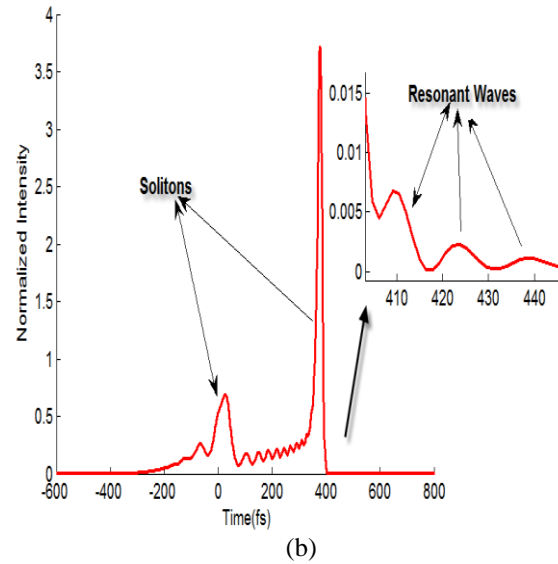
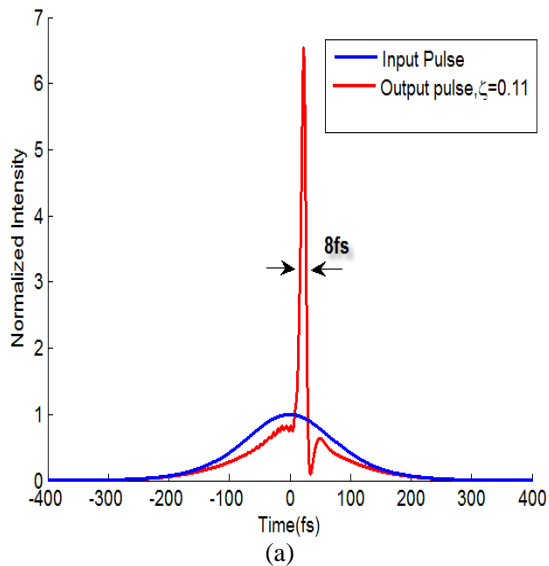


Fig. 8. Simulated evolution of the optical pulse after:
 a) $\xi = 0.11$, b) $\xi = 0.22$, c) $\xi = 0.55$. The input pulse is also shown

6. CONCLUSION

In this article, initially the design of a PCF with ideal conditions for nonlinear applications especially super continuum generation (SCG) and compression of optical pulses by applying full vector multi pole method based on using the CUDOS MOF software in low loss wavelength of 1310nm is investigated. It was shown that by adjusting the geometrical parameters of the PCF such as pitch (Λ) and normalized air holes diameter ($\frac{d}{\Lambda}$), we can centralize a minimum and nearly flat region of large negative GVD at 1310nm and finally calculate the smaller higher-order dispersions which are ideally needed for efficient

soliton-effect compression of the optical pulses and super continuum generation. Compared to the other structures of silica PCF, this structure has a larger nonlinear coefficient ($\gamma = 80(W.Km)^{-1}$) and also requires less amount of energy for nonlinear applications. By using a 100fs input pulse with a low energy of 1056pJ (corresponds to peak power of 5280watt), a compressed laser pulse of 8fs can be obtained for a silica PCF with considering

$$\Lambda = 1.38\mu m \quad \text{and} \quad \frac{d}{\Lambda} = 0.8 \quad \text{at the normalized}$$

propagation distance of $\zeta = 0.11$. Moreover, by taking the linear and nonlinear effects on generated super continuum spectrum at discrete locations into consideration, it generally is revealed that in silica PCF, Raman effect in comparison with other effects is dominant. But, in propagation of femtosecond optical pulses, applying the self-steepening (S.S) effect is also important in a way that, this effect leads to transferring the spectrum towards lower wavelengths and also raising the spectrum magnitude. It is also noted that using dispersions effects result in further spread of the pulses and generated spectrum. Consequently, ideal engineering of PCFs for the purpose of reducing higher order dispersions (HODs), as was followed in this article, is absolutely essential.

REFERENCES

- [1] R. V. J. Raja, K. Porsezian, S. K. Varshney, and S. Sivabalan, "Modeling photonic crystal fiber for efficient soliton pulse propagation at 850nm" *Elsevier, Optic Communications*, pp. 5000-5006, 2010.
- [2] M. V. Tognetti, "Sub two-cycle soliton-effect pulse compression at 800nm in photonic crystal fibers", *Optics Infobase*, Vol. 24, Issue. 6, Jun.1, 2007.
- [3] M. F. S. Ferreira, "Nonlinear effects in optical fibers", Wiley, 2011.
- [4] R. Cherif, M. Zghal, "Nonlinear phenomena of ultra-wide-band radiation in photonic crystal fiber", *Hindawi publication production*, pp. 1-6, Vol. 2011, Article ID 374581, 2011.
- [5] S. K. Singh, D. K. Singh, P. Mahto, "Numerical analysis of dispersion and endlessly single mode property of a modified photonic crystal fiber structure", *Int. J. Advanced Networking and Applications*, Vol. 03, Issue. 02, pp. 116-1120, Jun.25, 2011.
- [6] K. Saitoh, M. Kushiba, "Numerical Modeling of Photonic Crystal Fibers", *J of Lightwave Technology*, Vol. 3, No. 11, November, 2005.
- [7] K. Saitoh, M. Kushiba, "Emprical relaitions for simple design of photonic crystal fibers", *Opt. Exp.*, Vol. 13, No. 1, pp. 267-274, 2005.
- [8] C. Hao, Z. X. Min, S. L. Fang, "Design of photonic crystal fibers with anomalous dispersion", *Opto-electron. lett*, 2006.
- [9] Z. K. Varallayay, "Nonlinear wave propagation and ultrashort pulse compression in step index and microstructured fibers", *PHD Thesis*, Budapest University of Technolgy and Economics Atomic Physics Department, 2007.
- [10] H. Saghaei, K. M. farshi, F. Dehghan, "Supercontinuum Generation in Photonic Crystal Fiber Using Selective Optofluidic infiltration", *ICOP, Tabriz, Iran*, pp. 106-110, 2012.
- [11] Z. Xia, X. Y. Zhao, H. Y. Qing, R. X. Min, "1.55um supercontinuum based on dispersion flattened photonic crystal fiber", *Opto-electronic Lett*, Vol. 3, No. 5, pp.0346-0348, 2007.
- [12] W. Chen, J. P. L. Li, "Progress of photonic crystal fibers and their applications", *Opto. electron. China*, Vol. 2, No. 1, pp.50-57, 2009.
- [13] A. V. Husakou, J. Herrmann, "Supercontinuum generation in photonic cyestal fibers from highly non-linear glasses", *Appl. Phys. B* 77, pp. 227-234, 2003.
- [14] F. Polli, S. Slleri, "Photonic crystal fibers applications and properties", springer, 2008.
- [15] H. Demir, S. Ozsoy, " Comparative Study of Large-Solid-Core Photonic Crystal Fibers: Dispersion and effective mode area", *Elsevier*, pp.1-5, 2011.
- [16] V. L. Kalashnikov, E. Sorokin, I. T. Sorokina, "Raman effects in the infrared supercontinuum generation in soft-glass photonic crystal fibers", *Apply. Phys. B*, pp. 37-44, 2007.
- [17] V. V. Ravi Kanth Kumar, A. K. George, W. H. Reeves, J. C. Knight, P. St. J. Russell, "Extruded soft glass photonic crystal fber for ultrabroad supercontinuum generation", *Opt. Exp*, Vol. 10, No. 25, pp. 1520-1526, 2002.
- [18] K. Saitoh and M. Koshiba, "Highly nonlinear dispersion flattened photonic crystal fibers for supercontinuum generation in a tele -communication window", *Opt. Exp*, Vol. 12, No. 10, pp. 2027-2033, 2004.
- [19] G. P. Agrawal, "Nonlinear fiber optics", 4th edition, Academic press, 2007.
- [20] C. C. Feng, C. Sien, "Femtosecond second order solitons in optical fiber transmtion", *Elsevier*, pp. 331-335, 2005.
- [21] M. Yichang, Z. Shumin, C. Jin, "Enhanced compression of femtosecond pulse in hollow core photonic band gap fibers", *Elsevier*, pp. 2411-2 415, 2005.
- [22] Z. Zhuman, T. G. Brown, "Effect of frequency chirping on supercontinuum generation in photonic crystal fibers", *Opt. Exp*, Vol. 12, No. 4, pp. 13203-13206, 2004.
- [23] V. C. Long, H. N. Viet, M. Tripenbach, "Propagation technique for ultrashort pulses", *CMST Journal*, 2008.
- [24] S. K. Varshney, R. K. Sinah, M. P. Singh, "Propagation characteristics of photonic crystal fibers", *J. Opt, Comm*, 2003.